ISSN 2231-346X (Print)
JUSPS-A Vol. 30(2), 129-142 (2018). Periodicity-Monthly
Section A
(Online) ISSN 2319-8044

JOURNAL OF ULTRA SCIENTIST OF PHYSICAL SCIENCES
An International Open Free Access Peer Reviewed Research Journal of Mathematics
website:- www.ultrascientist.org
Estd. 1989

Numerical Study of Natural Convection in a Square Cavity with Magnetic field and Semi Circular Heat Source of Different Orientations

A. SHAREEF[1], and R. SIVA PRASAD[2]

[1]Research Scholar, Department of Mathematics, Rayalaseema University, Kurnool, Andhra Pradesh 518007 (India)
[2]Department of Mathematics, Sri Krishnadevaraya University, Anantapuram, Andhra Pradesh 515003 (India)
Corresponding author Email: shareef.maths@gmail.com
http://dx.doi.org/10.22147/jusps-A/300204

Acceptance Date 14th January, 2018, Online Publication Date 2nd February, 2018

Abstract

The effects of MHD free convection on heat flow within a square cavity. Free convection flow in the presence of magnetic field in a square cavity with semi circular heat source is studied in this paper. The lower wall of cavity is heated from below and the upper wall of cavity is cold; on the other hand, the side walls of the cavity are thermally insulated.

In the current study, Finite Element Method has been used to convert the non-linear coupled partial differential equations for flow and temperature field into a matrix form of equations, which can be solved iteratively with the help of a computer code. The Galerkin Finite Element Method of three nodded triangular elements is used to divide the physical domain into smaller segments, which is a pre-requisite for finite element method. Numerical results are presented in terms of stream functions, isotherms, temperature profiles and Nusselt numbe.

Key words: Viscous fluid, Heat transfer, Convection, Finite element methods.
Subject Classification Codes 2010:76DXX, 35Q79, 76E06, 74S05.

1. Introduction

Free convection in cavity has received considerable attention from researchers. Most of the cavities commonly used in industries are circular, square, rectangular, trapezoidal and triangular etc. Square cavities

have received a considerable attention for its application in various fields Swastik Acharya , Sukanta K Dash[1], Natural Convection Heat Transfer From a Short or Long, Solid or Hollow Horizontal Cylinder Suspended in Air or Placed on Ground Interesting flow structures around the thin hollow cylinder ,have been observed for small and large L/D. It has been found that the average Nu for solid or hollow horizontal cylinders in air is marginally higher than when they are on ground for the entire range Thirupathi Thumma, A. hamkha, Siva Reddy Sheri,[2] MHD natural convective flow of nanofluids past stationary and moving inclined porous plate considering temperature and concentration gradients with suction, they observed that an increase of suction reduces the heat and mass transfer. M.A.Taghikhani and H.R.Chavoshi[3] numerically investigated two dimensional magneto hydrodynamics (MHD) free convection with internal heating in a square cavity. They observed that the effect of the magnetic field is to reduce the convective heat transfer inside the cavity. Y.Bakhshan and H.Ashoori[4] investigated numerically analysis of a fluid behavior in a rectangular enclosure under the effect of magnetic field. They observed that Nusselt number rises with increasing Grashof and Prandtl numbers and decreasing Hartmann and orientation of magnetic field. F. HakanÖztop and Al-Salem[5] numerically investigated effects of joule heating on MHD natural convection in non-isothermally heated enclosure. They observed that positive stream functions are decreased with increasing of Hartmann number and thermal boundary layer becomes larger. S. Parvin and R, Nasrin[6] investigated numerically analysis of the flow and heat transfer characteristics for MHD free convection in an enclosure with a heated obstacle. They found that buoyancy-induced vortex in the streamlines is increased and thermal layer near the heated surface becomes thick with increasing Rayleigh number. Natural convection in a square cavity localized heating from below was investigated by B.Santosh,Aswatha and K.N.Seetharamu *et al*.[7]. They observed that heat transfer increases when the heater source is placed towards the cold wall.

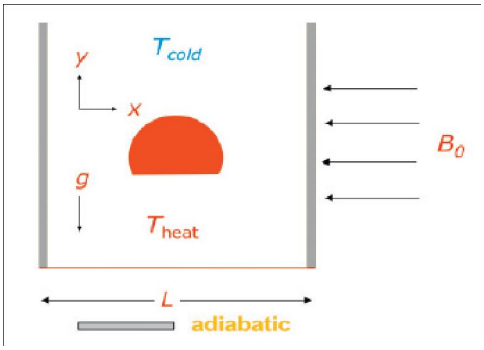

Fig.1: Schematic diagram of the physical system.

2. Mathematical Formulation:

A schematic diagram of the system considered in present study is shown in Fig. 1. The system consists of a square cavity with sides of length L and a semi-circular solid block is located at the centre of the enclosure. The left and right walls are considered to be adiabatic. The top wall is kept at a constant temperature Tc . The bottom wall and semi-circular obstacle are assumed to be uniform temperature be Th. Here Tc is less than Th. The uniform magnetic field B_0 is also applied to the fluid in the direction parallel to y. Based on the model, two dimensional, laminar, incompressible steady equations are written by considering a uniform applied magnetic field. The gravitational force (g) acts in the vertically downward direction. We assumed that Boussinesq approximation is valid and radiation mode of the heat transfer and Joule heating are neglected. Thus, using the coordinate system shown in Fig. 1, the governing equations can be written in dimensional form

$$\frac{\partial u}{\partial x}+\frac{\partial v}{\partial y}=0 \tag{3.1}$$

$$\rho\left(u\frac{\partial v}{\partial x}+v\frac{\partial v}{\partial y}\right)=-\frac{1}{\rho}\frac{\partial p}{\partial y}+\vartheta\left(\frac{\partial^2 v}{\partial x^2}+\frac{\partial^2 v}{\partial y^2}\right)+g\beta(T-T_c)-B_0^2 v \tag{3.2}$$

$$u\frac{\partial T}{\partial x}+v\frac{\partial T}{\partial y}=\alpha\left(\frac{\partial^2 T}{\partial x^2}+\frac{\partial^2 T}{\partial y^2}\right) \tag{3.3}$$

with boundary conditions

u (x , 0) = u(x, L) =u(0 , y) = u(L , y) = 0,
v (x , 0) = v(x, L) = v(0 , L) = v(L , y) = 0,
T (x, 0) = T_h,

$$\frac{\partial T}{\partial y}(x,L)=0,\quad T(0,y)=T_h-(T_h-T_c)\frac{y}{L},$$

The Continuity equation (3.1) can be satisfied automatically by introducing the stream function 'ψ' as

$$u=\frac{\partial \psi}{\partial y} \tag{3.4a}$$

$$v=-\frac{\partial \psi}{\partial x} \tag{3.4b}$$

where x and y are the distances measured along the horizontal and vertical directions respectively u and v are the velocity components in the x and y directions respectively T denotes the temperature ϑ and α are kinematic viscosity and thermal diffusivity respectively P is the pressure and ρ is the density T_h and T_c are the temperatures at hot bottom wall and cold vertical wall respectively L is the side of the square cavity.
Using the following non dimensional variables,

Width $X=\frac{x}{L}$; Height $Y=\frac{y}{L}$

Velocity components $\begin{cases} U=\frac{uL}{\alpha} \\ V=\frac{vL}{\alpha} \end{cases}$; Stream function $\overline{\psi}=\frac{\psi}{\alpha}$

Pressure $P=\frac{pL^2}{\rho\alpha^2}$; Prandtl Number $\mathrm{Pr}=\frac{\nu}{\alpha}$;

Hartmann Number $Ha^2=\frac{B_0^2L^3}{\mu}$;

Rayleigh number $$Ra = \frac{g\beta(T_h - T_c)L^3 \Pr}{\nu^2} \quad ;$$

Temperature $$\theta = \frac{T - T_c}{T_h - T_c}$$

The governing equations (3.1)-(3.3) reduce to non-dimensional form as

$$\frac{\partial U}{\partial X} + \frac{\partial V}{\partial Y} = 0 \tag{3.5}$$

$$U\frac{\partial V}{\partial X} + V\frac{\partial V}{\partial Y} = -\frac{\partial P}{\partial Y} + \Pr\left(\frac{\partial^2 V}{\partial X^2} + \frac{\partial^2 V}{\partial Y^2}\right) + Ra\Pr\theta - Ha^2 \Pr V \tag{3.6}$$

$$U\frac{\partial \theta}{\partial X} + V\frac{\partial \theta}{\partial Y} = \left(\frac{\partial^2 \theta}{\partial X^2} + \frac{\partial^2 \theta}{\partial Y^2}\right) \tag{3.7}$$

with the non dimensionless boundary conditions are

$U(X, 0) = U(X, 1) = U(0, Y) = U(1, Y) = 0$; $V(X, 0) = V(X, 1) = V(0, Y) = V(1, Y) = 0$,

$\theta(X, 0) = 1$, $\frac{\partial \theta}{\partial Y}(X, 1) = 0$,

where X and Y are dimensionless coordinates varying along horizontal and vertical directions respectively U and V are dimensionless velocity components in the X and Y directions respectively θ is the dimensionless temperature P is the dimensionless pressure Ra and Pr are Rayleigh Prandtl numbers respectively.

3. Solution of Problem: Thus far we have derived the partial differential equations, which describe the heat and fluid flow behavior in the vicinity of porous medium. The development of governing equations is one part but the second and important part is to solve these equations in order to predict the various parameters of interest in the porous medium. There are various numerical methods available to achieve the solution of these equations, but the most popular numerical methods are Finite difference method, Finite volume method and the Finite element method. The selection of these numerical methods is an important decision, which is influenced by variety of factors amongst which the geometry of domain plays a vital role. Other factors include the ease with which these partial differential equations can be transformed into simple forms, the computational time required and the flexibility in development of computer code to solve these equations.In the present study, we have predominantly used Finite Element Method (FEM). The following sections enlighten the Finite element method and present its application to solve the above-mentioned equations.

The Finite Element Method is a deservingly popular method amongst scientific community. This method was originally developed to study the mechanical stresses in a complex airframe structure popularized by Zienkiewicz and Cheung (23) by applying it to continuum mechanics. Since then the application of Finite Element Method has been exploited to solve the numerous problems in various engineering disciplines. The great thing about finite element method is its ease with which it can be generalized to myriad engineering problems comprised of different materials.

Another admirable feature of the Finite Element Method (FEM) is that it can be applied wide range of geometries having irregular boundaries, which is highly difficult to achieve with other contemporary methods.

FEM can be said to have comprised of roughly 5 steps to solve any particular problem. The steps can be summarized as

- **Descritizing the domain:** This step involves the division of whole physical domain into smaller segments known as elements, and then identifying the nodes, coordinates of each node and ensuring proper connectivity between the nodes.
- **Specifying the equation:** In this step, the governing equation is specified and an equation is written in terms of nodal values
- **Development of Global matrix:** The equations are arranged in a global matrix which takes into account the whole domain
- **Solution:** The equations are solved to get the desired variable at each table in the domain
- **Evaluate the quantities of interest:** After solving the equations a set of values is obtained for each node, which can be further processed to get the quantities of interest.

There are varieties of elements available in FEM, which are distinguished by the presence of number of nodes. The present study is carried out by using a simple 3-noded triangular element as shown in fig. 2

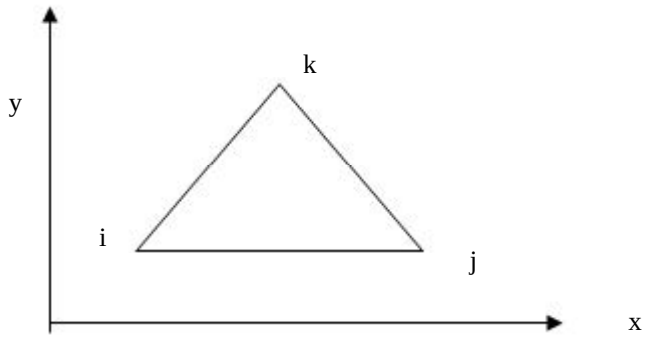

Fig. 2. Typical triangular element

Let us consider that the variable to be determined in the triangular area is 'θ'. The polynomial function for 'θ' can be expressed as:

$$\theta = \alpha_1 + \alpha_2 x + \alpha_3 y \tag{1}$$

The variable θ has the value θ_i, θ_j and θ_k at the nodal position i, j, and k of the element. The x and y coordinates at these points are x_i, x_j, x_k and y_i, y_j and y_k respectively. Substitution of these nodal values in the equation (1) helps in determining the constants α_1, α_2, α_3 which are:

$$\alpha_1 = {}^1/_{2A}\left[(x_j y_k - x_k y_j)\,\theta_i + (x_k y_i - x_i y_k)\,\theta_j + (x_i y_j - x_j y_i)\,\theta_k\right] \tag{2}$$

$$\alpha_2 = {}^1/_{2A}\left[(y_j - y_k)\,\theta_i + (y_k - y_i)\,\theta_j + (y_i - y_j)\,\theta_k\right] \tag{3}$$

$$\alpha_3 = {}^1/_{2A}\left[(x_k - x_j)\,\theta_i + (x_i - x_k)\,\theta_j + (x_j - x_i)\,\theta_{k_k}\right] \tag{4}$$

where A is area of the triangle given as

$$2A = \begin{vmatrix} 1 & x_i & y_i \\ 1 & x_j & y_j \\ 1 & x_k & y_k \end{vmatrix} \tag{5}$$

Substitution of α_1, α_2, α_3 in the equation (1) and mathematical arrangement of the terms results into

$$\theta = N_i \theta_i + N_j \theta_j + N_k \theta_k \tag{6}$$

In equation (6), N_i, N_j and N_k are the shape function given by

$$N_m = \frac{a_m + b_m x + c_m y}{2A}, \qquad m = i, j, k \tag{7}$$

The constants can be expressed in terms of coordinates as

$$a_i = x_j y_k - x_k y_j$$
$$b_i = y_j - y_k \tag{8a}$$
$$c_i = x_k - x_j$$
$$a_j = x_k y_i - x_i y_k$$
$$b_j = y_k - y_i \tag{8b}$$
$$c_j = x_i - x_k$$
$$a_k = x_i y_j - x_j y_i$$
$$b_k = y_i - y_j \tag{8c}$$
$$c_k = x_j - x_i$$

The triangular element can be subdivided into three triangles with a point in the center of original triangle as shown in fig. 3.

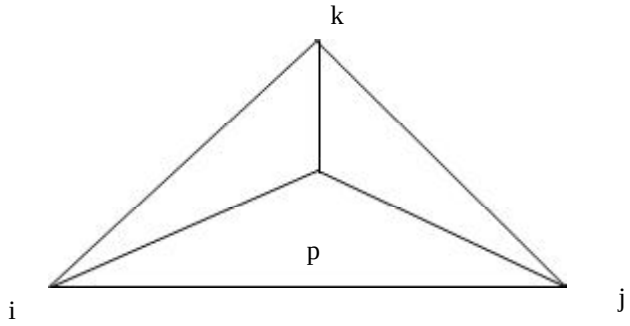

Fig. 3. showing the sub triangular areas

Defining the new area ratios as

$$L_1 = \frac{area\ \ pij}{area\ \ ijk} \tag{9a}$$

$$L_2 = \frac{area\ \ pjk}{area\ \ ijk} \tag{9b}$$

$$L_3 = \frac{area\ \ pki}{area\ \ ijk} \tag{9c}$$

It can be shown that

$$L_1 = N_1 \tag{10a}$$
$$L_2 = N_2 \tag{10b}$$
$$L_3 = N_3 \tag{10c}$$

Good insight into the FEM is given in Segerlind[24], Galerkin method is employed to convert the partial differential equations into matrix form for an element. The steps invented are as given below. Please note that the nodal terms *i, j & k* are replaced by 1,2 & 3 respectively in subsequent discussions for simplicity.

The momentum and energy balance equations are solved using the Galerkin finite element method. Continuity equation will be used as a constraint due to mass conservation and this constraint may be used to obtain the pressure distribution. In order to solve equations, we use the finite element method where the pressure P is eliminated by a penalty parameter γ and the incompressibility criteria given by equation (3.5) which results in

$$P = -\gamma \left(\frac{\partial U}{\partial X} + \frac{\partial V}{\partial Y} \right) \tag{3.8}$$

The continuity equation (3.5) is automatically satisfied for large values of γ.

Using equation (3.8) and introducing stream function, the momentum equation (3.6) reduce to

$$\left[\frac{\partial \overline{\psi}}{\partial Y} \frac{\partial^2 \overline{\psi}}{\partial X \partial Y} - \frac{\partial \overline{\psi}}{\partial X} \frac{\partial^2 \overline{\psi}}{\partial Y^2} \right] = \gamma \left(\frac{\partial^2 \overline{\psi}}{\partial Y^2} \frac{\partial \overline{\psi}}{\partial X} + \frac{\partial^2 \overline{\psi}}{\partial Y^2} \right) + \Pr \left[\frac{\partial^2 \overline{\psi}}{\partial X^2} + \frac{\partial^2 \overline{\psi}}{\partial Y^2} \right] - Ra \Pr \theta + Ha^2 \Pr \frac{\partial \overline{\psi}}{\partial Y} \tag{3.10}$$

Application of Galerkin method to equation (3.10) yields:

$$\left\{ R^e \right\} = -\int_A N^T \begin{Bmatrix} \left[\frac{\partial \overline{\psi}}{\partial Y} \frac{\partial^2 \overline{\psi}}{\partial X \partial Y} - \frac{\partial \overline{\psi}}{\partial X} \frac{\partial^2 \overline{\psi}}{\partial Y^2} \right] - \gamma \left(\frac{\partial^2 \overline{\psi}}{\partial Y^2} \frac{\partial \overline{\psi}}{\partial X} + \frac{\partial^2 \overline{\psi}}{\partial Y^2} \right) \\ - \Pr \left[\frac{\partial^2 \overline{\psi}}{\partial X^2} + \frac{\partial^2 \overline{\psi}}{\partial Y^2} \right] + Ra \Pr \theta - Ha^2 \Pr \frac{\partial \overline{\psi}}{\partial Y} \end{Bmatrix} dX dY \tag{3.11}$$

where R^e is the residue.
Considering the terms individually

$$\int_A [N]^T \frac{\partial \overline{\psi}}{\partial Y} \frac{\partial^2 \overline{\psi}}{\partial X \partial Y} dA = \frac{1}{4A} \begin{Bmatrix} c_1 \overline{\psi}_1 + c_2 \overline{\psi}_2 + c_3 \overline{\psi}_3 \\ c_1 \overline{\psi}_1 + c_2 \overline{\psi}_2 + c_3 \overline{\psi}_3 \\ c_1 \overline{\psi}_1 + c_2 \overline{\psi}_2 + c_3 \overline{\psi}_3 \end{Bmatrix} \left[b_1, b_2, b_3 \right] \tag{3.12}$$

$$\int_A [N^T] \frac{\partial \overline{\psi}}{\partial X} \frac{\partial^2 \overline{\psi}}{\partial Y^2} dA = \frac{1}{12A} \begin{Bmatrix} b_1 \overline{\psi}_1 + b_2 \overline{\psi}_2 + b_3 \overline{\psi}_3 \\ b_1 \overline{\psi}_1 + b_2 \overline{\psi}_2 + b_3 \overline{\psi}_3 \\ b_1 \overline{\psi}_1 + b_2 \overline{\psi}_2 + b_3 \overline{\psi}_3 \end{Bmatrix} \left[c_1, c_2, c_3 \right] \tag{3.13}$$

$$\int_A [N^T] \gamma \frac{\partial^2 \overline{\psi}}{\partial Y^2} \frac{\partial \overline{\psi}}{\partial X} dA = \frac{\gamma}{12A} \begin{Bmatrix} b_1 \overline{\psi}_1 + b_2 \overline{\psi}_2 + b_3 \overline{\psi}_3 \\ b_1 \overline{\psi}_1 + b_2 \overline{\psi}_2 + b_3 \overline{\psi}_3 \\ b_1 \overline{\psi}_1 + b_2 \overline{\psi}_2 + b_3 \overline{\psi}_3 \end{Bmatrix} \left[c_1, c_2, c_3 \right] \tag{3.14}$$

$$\int_A [N^T]\gamma \frac{\partial^2 \overline{\psi}}{\partial Y^2} dA = -\frac{\gamma}{4A}\begin{bmatrix} b_1^2 & b_1b_2 & b_1b_3 \\ b_1b_2 & b_2^2 & b_2b_3 \\ b_1b_3 & b_2b_3 & b_3^2 \end{bmatrix}\begin{bmatrix} \theta_1 \\ \theta_2 \\ \theta_3 \end{bmatrix} \tag{3.15}$$

$$\int_A [N^T]\Pr \frac{\partial^2 \overline{\psi}}{\partial X^2} dA = -\frac{\Pr}{4A}\begin{bmatrix} c_1^2 & c_1c_2 & c_1c_3 \\ c_1c_2 & c_2^2 & c_2c_3 \\ c_1c_3 & c_2c_3 & c_3^2 \end{bmatrix}\begin{bmatrix} \theta_1 \\ \theta_2 \\ \theta_3 \end{bmatrix}$$

$$\int_A [N^T]\Pr \frac{\partial^2 \overline{\psi}}{\partial Y^2} dA = -\frac{\Pr}{4A}\begin{bmatrix} b_1^2 & b_1b_2 & b_1b_3 \\ b_1b_2 & b_2^2 & b_2b_3 \\ b_1b_3 & b_2b_3 & b_3^2 \end{bmatrix}\begin{bmatrix} \theta_1 \\ \theta_2 \\ \theta_3 \end{bmatrix} \tag{3.16}$$

$$\int_A [N]^T RaP\theta dA = \frac{RaP}{12A}\begin{bmatrix} \theta_1 \\ \theta_2 \\ \theta_3 \end{bmatrix} \tag{3.17}$$

$$\int_A [N^T]Ha^2 \Pr \frac{\partial \overline{\psi}}{\partial Y} dA = \frac{Ha^2 \Pr}{4A}\begin{bmatrix} b_1^2 & b_1b_2 & b_1b_3 \\ b_1b_2 & b_2^2 & b_2b_3 \\ b_1b_3 & b_2b_3 & b_3^2 \end{bmatrix}\begin{bmatrix} \theta_1 \\ \theta_2 \\ \theta_3 \end{bmatrix} \tag{3.17}$$

Thus the whole equation (3.10) can be written in matrix form as

$$\frac{1}{4A}\begin{Bmatrix} c_1\overline{\psi}_1 + c_2\overline{\psi}_2 + c_3\overline{\psi}_3 \\ c_1\overline{\psi}_1 + c_2\overline{\psi}_2 + c_3\overline{\psi}_3 \\ c_1\overline{\psi}_1 + c_2\overline{\psi}_2 + c_3\overline{\psi}_3 \end{Bmatrix}[b_1, b_2, b_3] - \frac{1}{12A}\begin{Bmatrix} b_1\overline{\psi}_1 + b_2\overline{\psi}_2 + b_3\overline{\psi}_3 \\ b_1\overline{\psi}_1 + b_2\overline{\psi}_2 + b_3\overline{\psi}_3 \\ b_1\overline{\psi}_1 + b_2\overline{\psi}_2 + b_3\overline{\psi}_3 \end{Bmatrix}[c_1, c_2, c_3]$$

$$+\frac{\gamma}{12A}\begin{Bmatrix} b_1\overline{\psi}_1 + b_2\overline{\psi}_2 + b_3\overline{\psi}_3 \\ b_1\overline{\psi}_1 + b_2\overline{\psi}_2 + b_3\overline{\psi}_3 \\ b_1\overline{\psi}_1 + b_2\overline{\psi}_2 + b_3\overline{\psi}_3 \end{Bmatrix}[c_1, c_2, c_3] + \frac{\gamma}{4A}\begin{bmatrix} b_1^2 & b_1b_2 & b_1b_3 \\ b_1b_2 & b_2^2 & b_2b_3 \\ b_1b_3 & b_2b_3 & b_3^2 \end{bmatrix}\begin{bmatrix} \theta_1 \\ \theta_2 \\ \theta_3 \end{bmatrix}$$

$$-\frac{\Pr}{4A}\begin{bmatrix} c_1^2 & c_1c_2 & c_1c_3 \\ c_1c_2 & c_2^2 & c_2c_3 \\ c_1c_3 & c_2c_3 & c_3^2 \end{bmatrix}\begin{bmatrix} \theta_1 \\ \theta_2 \\ \theta_3 \end{bmatrix} + -\frac{\Pr}{4A}\begin{bmatrix} b_1^2 & b_1b_2 & b_1b_3 \\ b_1b_2 & b_2^2 & b_2b_3 \\ b_1b_3 & b_2b_3 & b_3^2 \end{bmatrix}\begin{bmatrix} \theta_1 \\ \theta_2 \\ \theta_3 \end{bmatrix}$$

$$+\frac{RaP}{12A}\begin{bmatrix}\theta_1\\ \theta_2\\ \theta_3\end{bmatrix}-\frac{Ha^2\,\mathrm{Pr}}{4A}\begin{bmatrix}b_1^2 & b_1b_2 & b_1b_3\\ b_1b_2 & b_2^2 & b_2b_3\\ b_1b_3 & b_2b_3 & b_3^2\end{bmatrix}\begin{bmatrix}\theta_1\\ \theta_2\\ \theta_3\end{bmatrix}=0 \tag{3.18}$$

Introducing stream function, the energy equation (3.7) reduces as

$$\frac{\partial\overline{\psi}}{\partial Y}\frac{\partial\theta}{\partial X}+\frac{\partial\overline{\psi}}{\partial X}\frac{\partial\theta}{\partial Y}=\left(\frac{\partial^2\theta}{\partial X^2}+\frac{\partial^2\theta}{\partial Y^2}\right) \tag{3.19}$$

FEM of Energy Equation is

$$\left\{R^e\right\}=-\int_A[N]^T\left(\frac{\partial\overline{\psi}}{\partial Y}\frac{\partial\theta}{\partial X}+\frac{\partial\overline{\psi}}{\partial X}\frac{\partial\theta}{\partial Y}-\frac{\partial^2\theta}{\partial X^2}-\frac{\partial^2\theta}{\partial Y^2}\right)dA \tag{3.20}$$

Considering the terms individually

$$\int_A[N]^T\frac{\partial\overline{\psi}}{\partial Y}\frac{\partial\overline{\theta}}{\partial X}dA=\frac{1}{12A}\begin{Bmatrix}c_1\overline{\psi}_1+c_2\overline{\psi}_2+c_3\overline{\psi}_3\\ c_1\overline{\psi}_1+c_2\overline{\psi}_2+c_3\overline{\psi}_3\\ c_1\overline{\psi}_1+c_2\overline{\psi}_2+c_3\overline{\psi}_3\end{Bmatrix}\begin{bmatrix}b_1,b_2,b_3\end{bmatrix}\begin{bmatrix}\theta_1\\ \theta_2\\ \theta_3\end{bmatrix} \tag{3.21}$$

$$\int_A[N^T]\frac{\partial\overline{\psi}}{\partial X}\frac{\partial\theta}{\partial Y}dA=\frac{1}{12A}\begin{Bmatrix}b_1\overline{\psi}_1+b_2\overline{\psi}_2+b_3\overline{\psi}_3\\ b_1\overline{\psi}_1+b_2\overline{\psi}_2+b_3\overline{\psi}_3\\ b_1\overline{\psi}_1+b_2\overline{\psi}_2+b_3\overline{\psi}_3\end{Bmatrix}\begin{bmatrix}c_1,c_2,c_3\end{bmatrix}\begin{bmatrix}\theta_1\\ \theta_2\\ \theta_3\end{bmatrix} \tag{3.22}$$

$$\int_A[N^T]\frac{\partial^2\theta}{\partial X^2}dA=-\frac{1}{4A}\begin{bmatrix}b_1^2 & b_1b_2 & b_1b_3\\ b_1b_2 & b_2^2 & b_2b_3\\ b_1b_3 & b_2b_3 & b_3^2\end{bmatrix}\begin{bmatrix}\theta_1\\ \theta_2\\ \theta_3\end{bmatrix} \tag{3.23}$$

$$\int_A[N^T]\frac{\partial^2\theta}{\partial Y^2}dA=-\frac{1}{4A}\begin{bmatrix}c_1^2 & c_1c_2 & c_1c_3\\ c_1c_2 & c_2^2 & c_2c_3\\ c_1c_3 & c_2c_3 & c_3^2\end{bmatrix}\begin{bmatrix}\theta_1\\ \theta_2\\ \theta_3\end{bmatrix} \tag{3.24}$$

Thus the whole equation (3.19) can be written in matrix form as

$$\frac{1}{12A}\begin{Bmatrix}c_1\overline{\psi}_1+c_2\overline{\psi}_2+c_3\overline{\psi}_3\\ c_1\overline{\psi}_1+c_2\overline{\psi}_2+c_3\overline{\psi}_3\\ c_1\overline{\psi}_1+c_2\overline{\psi}_2+c_3\overline{\psi}_3\end{Bmatrix}\begin{bmatrix}b_1,b_2,b_3\end{bmatrix}\begin{bmatrix}\theta_1\\ \theta_2\\ \theta_3\end{bmatrix}-\frac{1}{12A}\begin{Bmatrix}b_1\overline{\psi}_1+b_2\overline{\psi}_2+b_3\overline{\psi}_3\\ b_1\overline{\psi}_1+b_2\overline{\psi}_2+b_3\overline{\psi}_3\\ b_1\overline{\psi}_1+b_2\overline{\psi}_2+b_3\overline{\psi}_3\end{Bmatrix}\begin{bmatrix}c_1,c_2,c_3\end{bmatrix}\begin{bmatrix}\theta_1\\ \theta_2\\ \theta_3\end{bmatrix}$$

$$-\frac{1}{4A}\begin{bmatrix} b_1^2 & b_1b_2 & b_1b_3 \\ b_1b_2 & b_2^2 & b_2b_3 \\ b_1b_3 & b_2b_3 & b_3^2 \end{bmatrix}\begin{bmatrix}\theta_1\\ \theta_2\\ \theta_3\end{bmatrix}+\frac{1}{4A}\begin{bmatrix} c_1^2 & c_1c_2 & c_1c_3 \\ c_1c_2 & c_2^2 & c_2c_3 \\ c_1c_3 & c_2c_3 & c_3^2 \end{bmatrix}\begin{bmatrix}\theta_1\\ \theta_2\\ \theta_3\end{bmatrix}=0 \tag{3.25}$$

4. Nusslet Number:

The average dimensionless Nusselt Number ($\overline{Nu}$) can be evaluated using the formula

$$\overline{Nu}=-\frac{\partial\theta}{\partial n} \tag{3.26}$$

where n denotes the normal direction on a plane.

5. Results and Discussion

A numerical analysis has been performed in this work to investigate the effects of magnetic field in a square cavity with a semi circular heated obstacle of different orientation parameter (rot). The ranges rot and Ha for this investigation vary from 0^0 to 90^0 and 0^0 to 100^0 respectively whereas other parameters are fixed at Ra = 10^4 and Pr = 0.71. In this section the influence of the Hartmann number (Ha = 0, 50,100) on the flow and temperature fields for Ra=10^4 and three values of the orientation parameter (rot=0^0, 60^0,90^0) are presented. Fig.4 illustrates the streamlines and isotherms for rot=0^0, where the buoyancy effects dominate the flow field in the cavity and the heat transfer is mainly due to natural convection. The results show that the buoyancy induced vortices in the cavity in the absence of the magnetic field (Ha = 0). Four vortices are evident inside of the cavity for Ha = 0. When the Hartmann number increases, both of them are vanished due to the effect of the magnetic field. The isotherms distribution is also affected by the effect of the magnetic field. Less bend of the isotherms lines is observed as the Hartmann number increases. Fig. 5 shows the streamlines and isotherms for rot=60^0. In the absence of the magnetic field, one vortex is appearing clearly right side of the heated body due to buoyancy force. As the Hartmann number increases size of the vortex larger and move to the top side and another vortex created on the left top corner. Bending of the isotherms lines are a lesser amount of with increasing Hartmann number.

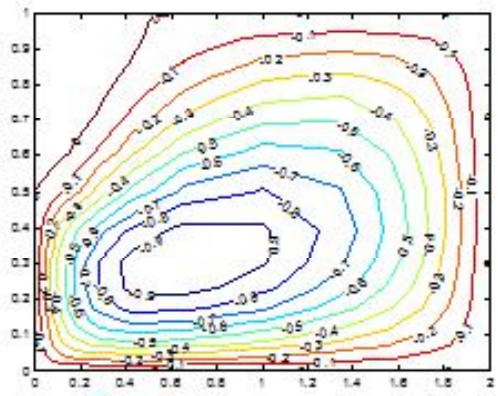

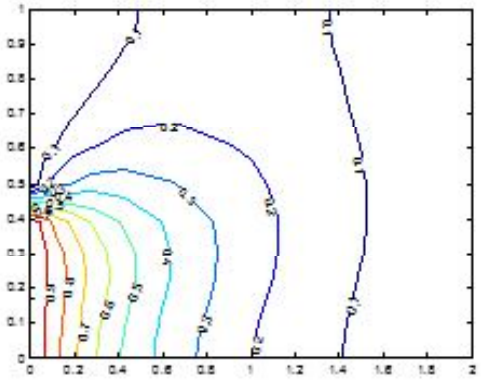

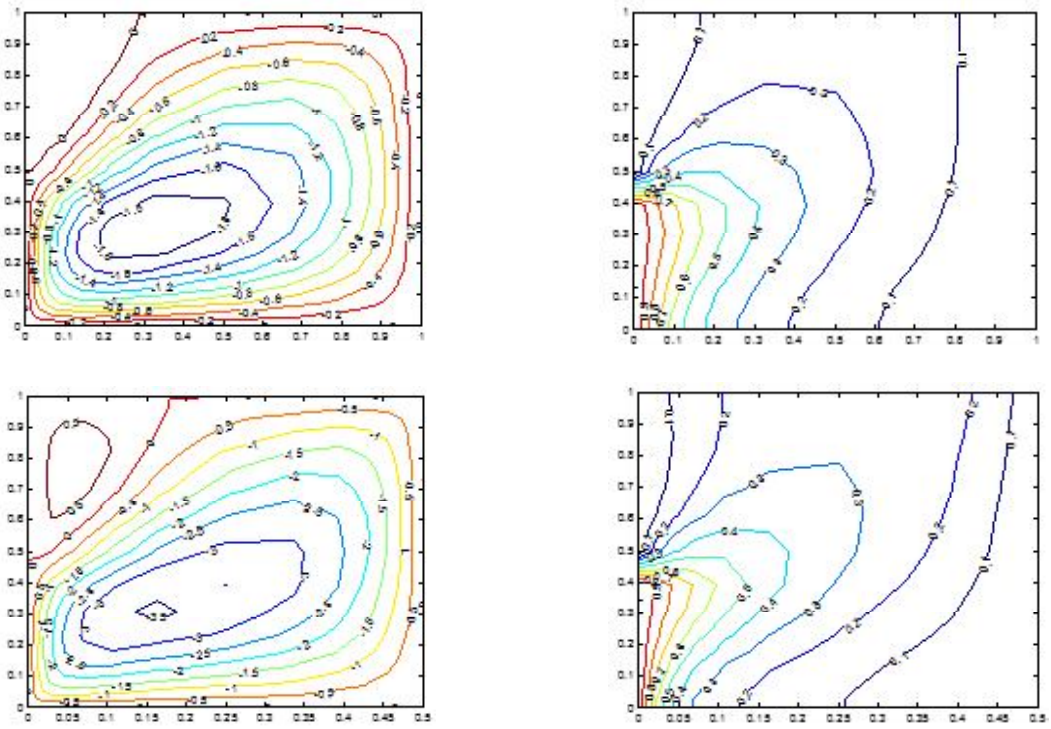

Fig. 4. Clockwise and anti-clockwise flows are shown via negative and positive signs of stream functions (Left) and Isotherms (Right) for rotation 0^0 with Pr = 0.71 and Ra=10000.

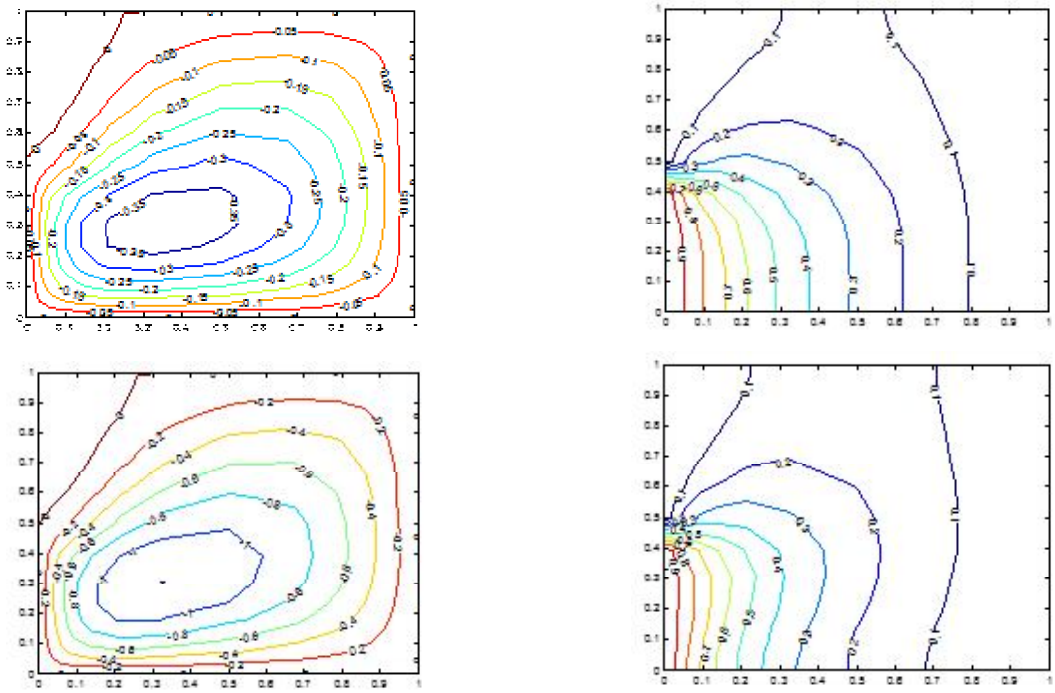

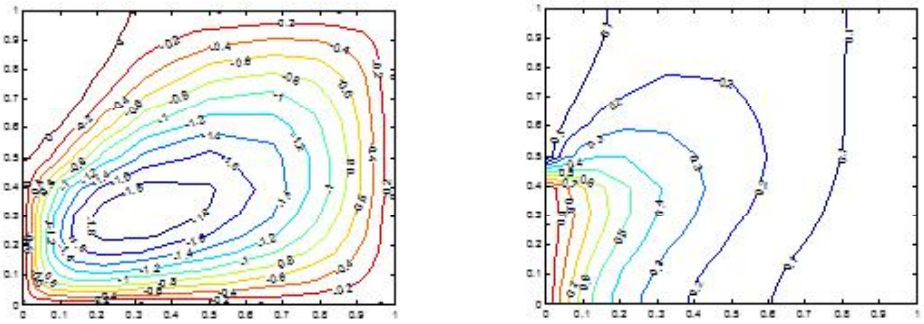

Fig. 5. Clockwise and anti-clockwise flows are shown via negative and positive signs of stream functions (Left) and Isotherms (Right) for rotation 60^0 with Pr=0.71 and Ra=10000.

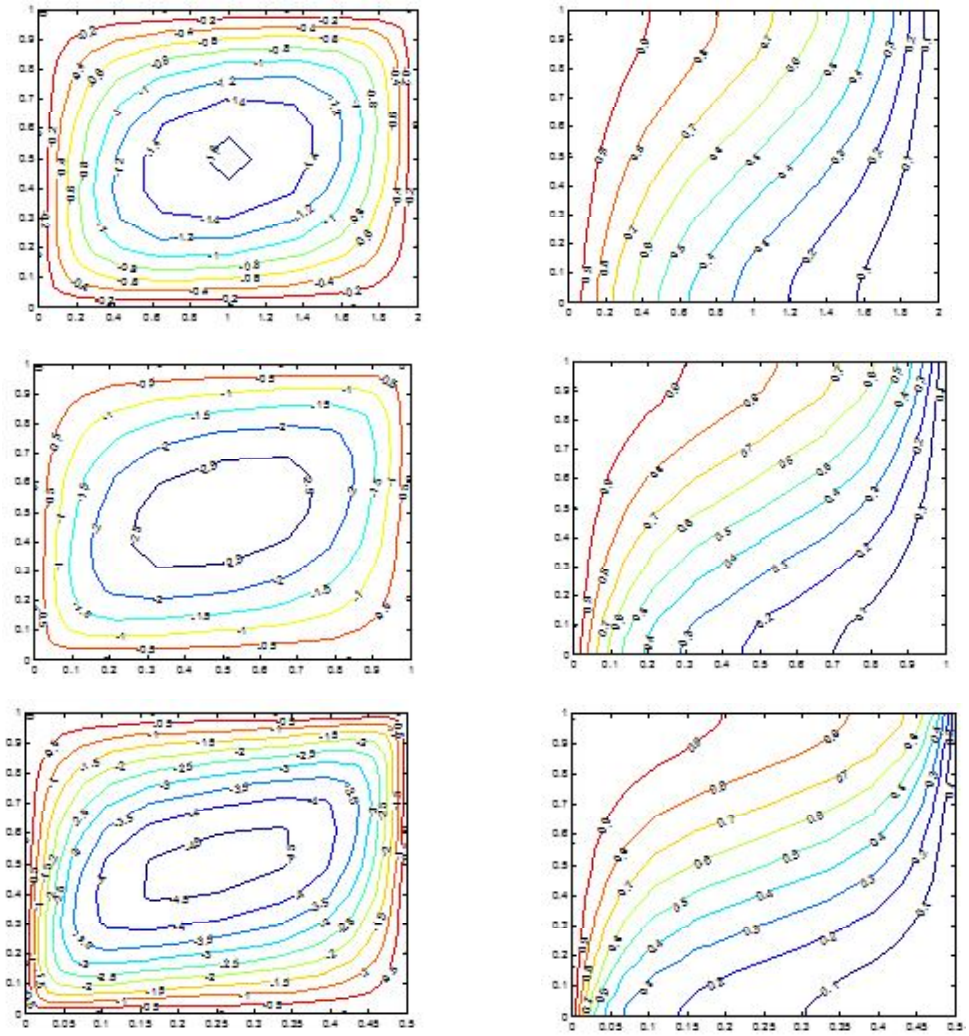

Fig. 6. Clockwise and anti-clockwise flows are shown via negative and positive signs of stream functions (Left) and Isotherms (Right) for rotation 90^0 with Pr=0.71 and Ra=10000.

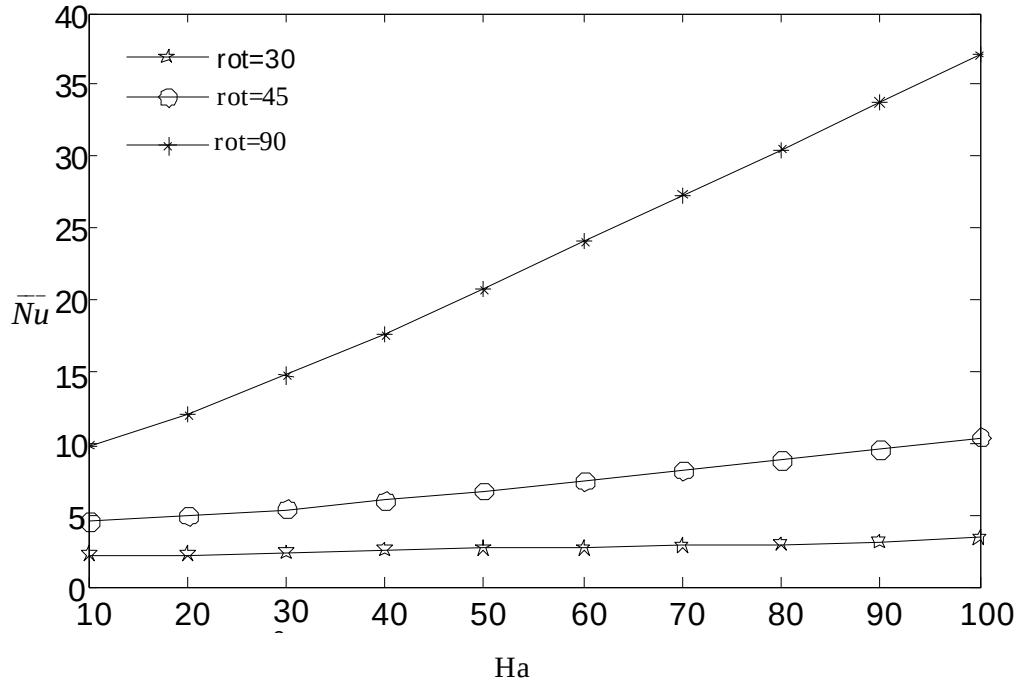

Fig. 7. Effect of Ha and rot on $\overline{Nu}$ while Pr = 0.71 and Ra = 10^4

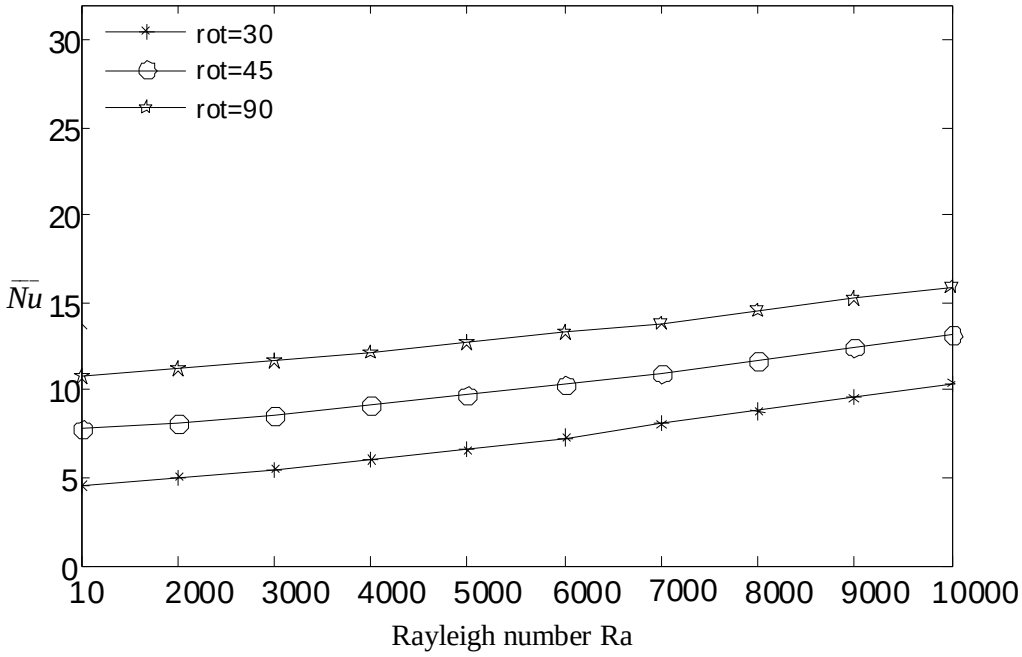

Fig. 8. Effect of Ra and rot on $\overline{Nu}$ while Pr = 0.71 and Ha = 0

Fig. 6 shows the streamlines and isotherms for rot = 90^0. In the absence of the magnetic field, elliptic size only one vortex is generated right side of the heated body due to buoyancy force. As the Hartmann number increases shape of the vortex seems to be almost circular and move to the top side and another vortex created on the left top corner. Effect of the magnetic field is also significant for isotherms lines. The average Nusselt number is plotted as a function of Hartmann number and Rayleigh number respectively as shown in Fig. 7 and Fig. 8 for five different orientation (rot = 0^0, 15^0, 30^0, 45^0, 90^0) while Pr = 0.71. The maximum heat transfer rate is obtained for the lowest Ha. This is because the magnetic field retards the flow.

6. Conclusion

The effects of magnetic field parameter Ha due to semi circular heat source, Prandtl number Pr and Rayleigh number Ra on flow and temperature field have been studied in detail. From the present investigation the following conclusions may be drawn: if Hartman number increases the Nusselt number, representing heat transfer from the cavity decreases and if Rayleigh number increases the Nusselt number increases.

7. Scope of future work :

Study the natural convection in a configurations of annulus cone, cylindrical cone, rectangular cone, trapezoidal cavity field etc. with radiation effects.

8. References

1. Swastik Acharya, Sukanta K Dash, Natural Convection Heat Transfer From a Short or Long, Solid or Hollow Horizontal Cylinder Suspended in Air or Placed on Ground *J. Heat Transfer* 139(7), 072501 (Mar 21,017) Paper No: HT-16-1792.
2. Thirupathi Thumma, A. Chamkha, Siva Reddy Sheri, "MHD natural convective flow of nanofluids past stationary and moving inclined porous plate considering temperature and concentration gradients with suction", International Journal of Numerical Methods for Heat & Fluid Flow, Vol. 27 Issue: 8, pp.1765-1794 (2017).
3. M.A. alim, M. A. Taghikhani, H. R. Chavoshi, Two dimensional MHD free convection with internal heating in a square cavity, Thermal Energy and Power Engineering, vol. *2*, pp. 22-28, (2013).
4. Y. Bakhshan, H. Ashoori, Analysis of a fluid behavior in a rectangular enclosure under the effect of magnetic field, World Academy of Science, Engineering and Technology, vol. 61, pp. 637- 641 (2012).
5. F. Hakan Öztop, Khaled Al-salem, Effects of joule heating on MHD natural convection in non-isothermally heated enclosure, J. of Thermal Science and Technology, vol. *32*, pp. 81-90 (2012).
6. S. Parvin, R. Nasrin, Analysis of the flow and heat transfer characteristics for MHD free convection in an enclosure with a heated obstacle, Nonlinear Analysis: Modeling and Control, vol. *16*, pp. 89–99 (2011).
7. B. Santosh, G. Archana, Aswatha, K. N. Seetharamu, Natural convection in a square cavity localized heating from below, The 37th National & 4th International Conference on Fluid Mechanics and Fluid Power December 16-18, 2010, IIT Madras, Chennai, India.
8. An introduction to Finite element method, Third edition, McGraw-Hill, New York (2005).